

Chapter 7. Telescope Structure

7.1 Introduction	7-2
7.1.1 Effects of Gravity Loads	7-2
7.1.2 Effects of Temperature Changes	7-3
7.1.3 Need for Active Control	7-3
7.1.4 Telescope Motion Control	7-4
7.1.5 Geometrical Tradeoffs	7-4
7.2 Primary Mirror Cell	7-5
7.2.1 General Objectives	7-5
7.2.2 Clusters	7-5
7.2.3 Cell and Subcell Topology	7-6
7.2.4 Cell Dimensions and Performance	7-8
7.2.5 Attachment to Elevation Journals	7-10
7.3 Secondary Support	7-11
7.4 Yoke	7-11
7.5 Telescope Performance	7-14
7.5.1 Static Deflections Against Gravity	7-14
7.5.2 Static Deflections Against Wind	7-20
7.5.3 Dynamics	7-22
7.6 Pier	7-23
7.7 Bearings	7-24
7.8 Drives and Encoders	7-24
7.9 Thermal Responses	7-25
7.10 Instrument Changing System	7-26
7.11 Segment Handling	7-26
7.12 IR Design Considerations	7-26
7.13 Control of Secondary and Tertiary	7-27
7.14 Field Rotation and Other Effects of Alt-Az Mount	7-27

7.1 Introduction

The telescope structure has the following main functions:

- Support the primary, secondary, and tertiary mirrors; the AO systems; and the instruments.
- Point the optical axis to any object in the sky and track it over time.
- Allow access for servicing the optics and instruments.
- Maintain support during operations against the expected changes in temperature, humidity, wind loads.
- Survive or operate in all expected environmental situations.
- Minimize the obscuration of light and the emission of thermal infrared radiation.

At this stage, the telescope structure design is incomplete. The design is based on the evolution of several intelligently selected approaches, but is not the result of an exhaustive investigation. We are currently optimizing the structure design to be consistent with many optical and mechanical constraints. We present here the current status and expect that major changes in the topology and geometry of the structure are likely to occur in the future.

The primary-secondary alignment requirements are roughly 0.1 mm (see Section 4.4.2), and segment support positioning requirements are under 100 nm. Ideally, we would like the structure alone to rigidly support the optics in their correct positions as it changes the direction of the optical axis and as its temperature changes. In practice, this is impossible. The next two sections calculate the rough magnitude of the gravity and temperature effects. We conclude from these calculations that active control of the optics is necessary.

7.1.1 Effects of Gravity Loads

Since gravity loads will vary as the telescope elevation angle changes, self-weight deflection of the structure will be at the very least (self-weight compression of a rod)

$$\delta = \rho g L^2 / (2E) \quad (7-1)$$

where δ is the deflection

g is the gravitational acceleration (9.8 m/s²)

ρ is the material density (for steel $\rho = 7.8 \times 10^3$ kg/m³)

L is the characteristic size of the structure (~ 50m)

E is the material elastic modulus (steel $E = 19.3 \times 10^{10}$ N/m²)

assuming the above values gives $\delta = 0.5$ mm. Any practical structure is likely to be 1-2 orders of magnitude worse than this.

For an additional example, consider a simply supported horizontal steel bar 50 m long and 10 m deep. It will deform 3.9 mm under its own weight. Deflections of structures like this grow as the 4th power of the length and inversely as the 2nd power of the depth.

These two static examples indicate the lower limit of the gravity driven effects. Designing a structure with varying gravity direction and with all the constraints of the telescope geometry will produce a structure that is inevitably more compliant than these static examples. A useful reference on the general gravity and thermal deformation limits is von Horner (1967).

7.1.2 Effects of Temperature Changes

Temperature changes will cause dimensional changes of

$$\delta = L\alpha\Delta T \quad (7-2)$$

where α is the coefficient of thermal expansion of the material (steel $\alpha = 1.2 \times 10^{-5} / ^\circ\text{C}$)
 ΔT is the temperature change.

Consider an example where the temperature changes by 10°C . In this circumstance the outermost segments will move radially by $\delta \sim 1.8$ mm. For the optical design of CELT, such motions are optically unimportant.

Temperature gradients also cause dimensional changes. For a single material the dimensional changes will be stress free. For a constant gradient of temperature experienced by a homogeneous material, straight lines normal to the direction of the gradient are deformed into arcs of circles, where the radius of the circle is given by

$$R_T = 1 / (\alpha\nabla T) \quad (7-3)$$

As an example, if ∇T is $0.1^\circ\text{C}/\text{m}$, then for steel, $R_T = 833,000$ m. If we had such a temperature gradient along the optical axis, then the primary mirror structure would develop a temperature driven sag of $s = R^2 / 2R_T = 0.14$ mm. With active optics, this motion can be eliminated. Such a gradient perpendicular to the optical axis would cause the secondary to decenter by 1 mm. Again, with active optics this motion can be eliminated.

7.1.3 Need for Active Control

Thus we see that both thermal and gravitational disturbances will be sufficiently large that careful balancing of the effects of these disturbances in the structural design and active control of the optical element positions are desirable. Even if the segments are “floated” in some ideal fashion thermal deformations will require active control.

Traditionally, optical telescopes have had mechanical designs that passively balance the motions of the primary and secondary mirrors so they maintained good relative optical alignment. The Serrurier truss, initially developed for the Hale 5-m telescope, accomplished this. More modern telescopes have also implemented this idea. For CELT, the motions are sufficiently large that we believe that balancing will be impractical, and that active positioning of the optics will be required. Further, given the success of active control of optics in other facilities (Keck, Gemini, VLT) we accept that active control is practical and more affordable than fine tuning of the structure itself, and also far more effective. Thus for CELT we have made a key decision. We assume that the structure should be built for maximum stiffness (to minimize wind disturbances and improve motion control) and that balancing of optical motions will be achieved actively.

At Keck the primary mirror segment positions are actively controlled with edge sensors and actuators. This system has worked extremely well, and effectively makes a rigid mirror supported by a steel mirror cell. The actuators work against this stiff structure to hold the mirrors in their desired positions.

7.1.4 Telescope Motion Control

We expect it will take significantly longer to move CELT than it takes to move a smaller telescope such as Keck. The power required to move the telescope a given angular distance in a given time varies as L^5 (assuming the mass grows as L^3). In addition, natural structural frequencies are generally getting smaller as L^{-1} , so dynamical limitations become more important as the telescope grows in size.

7.1.5 Geometrical Trade-offs

Several optical parameters drive the structural design. The diameter of the primary mirror, the primary-secondary distance, the location of the elevation axis, the location of the final focus, and the associated instrument sizes are the most important.

In most previous optical telescopes, the primary mirror and its support cell form one end of what is commonly called the telescope tube, while the secondary mirror is held at the opposite end. A structure around the perimeter of the tube, containing the center of gravity of the tube, then forms the attachment to the rest of the structure, which is commonly called the base, yoke, or alidade. This connection forms a moving joint, and the motion defines the elevation axis. The yoke rotates about a vertical axis, relative to the telescope pier (fixed to the ground). These two rotation axes form the elevation-azimuth motion coordinate system.

For the design of larger telescopes, it is structurally advantageous to use a smaller focal ratio for the primary mirror. This is balanced by an increased difficulty in fabricating and aligning the optical surfaces. The Hale telescope is $f/3.3$, the Keck telescopes are $f/1.75$ and the current plan for CELT is $f/1.5$. In contrast, radio telescopes, with much coarser optical tolerances, are less difficult to fabricate and align, and use primary mirrors at $f/0.4$.

For shorter focal ratios, there are two design options worth considering. First, it becomes practical to consider placing the elevation axis behind the primary, rather than in front of it. When the light beam goes to a Nasmyth platform it is usually required that the elevation axis be significantly behind the primary, so the light beam outward along the elevation axis does not interfere with the support structure. Second, supporting the primary mirror directly behind the surface becomes more efficient than holding the tube only at its perimeter.

Radio telescopes typically place the elevation axis behind the primary, using counterweights to move the center-of-gravity to the elevation axis. This allows the primary mirror support structure to be efficiently developed directly behind the mirror itself. Because the focal length is so short, the size of an enclosure is driven by the diameter, not the length of the telescope.

For CELT we are in a transitional region. If the primary focal ratio were $f/1$ or less, it might be attractive to move the elevation axis behind the primary. However, at the moment we believe that optical fabrication and segment positioning difficulties preclude this solution. A study by Meinel and Meinel (2000) explores the possibilities of placing the elevation axis behind the primary.

We plan to directly support the primary and its cell from behind the cell and on the yoke, rather than carry the loads up through the perimeter of the tube and over to the yoke. Thus we plan to have large bearing surfaces directly behind the primary, to both transfer the load to the yoke and to define the elevation axis.

This kind of structure is not amenable to the design optimization methods of a Serrurier truss. We expect that the secondary support structure will be developed directly from the mirror cell and support bearing surfaces, rather than from an intermediate elevation ring.

7.2 Primary Mirror Cell

The primary mirror cell supports the primary mirror segments and carries their loads to the yoke. The cell is also responsible for attaching to the upper tube (the support structure for the secondary mirror) and carrying those loads back to the bearings that allow the motion around the elevation axis.

7.2.1 General Objectives

The mirror cell must adequately support the segments against the deforming influences of gravity and temperature changes. It must conveniently attach to the mirror segment system on one end and to the elevation bearings on the other. Since the cell deformations will be larger than the segment alignment tolerances, active control of the segment positions will be needed. Thus a key requirement of the mirror cell design is that its deformations be smooth and not exceed the motion range of the segment support actuators. The range about the average displacement is the key parameter. Currently we are designing the actuators to have a range of 2 mm. In-plane motions must also be limited since we do not plan to actively control these three degrees of freedom. This system has been very successful at Keck.

The upper parts of the mirror cell must allow accurate positioning of the segments, and also allow easy installation and removal of the segments. In addition, servicing requirements must be met, from periodic cleaning of the optical surfaces to replacement of broken segment support actuators and sensors.

We also want the mirror cell to have the lowest practical mass and to be designed for economy of construction and erection. The low mass will reduce the adverse impact on the thermal environment of the telescope and ease the requirements on the motion control system.

7.2.2 Clusters

In our reference optical design we have 1080 hexagonal mirror segments. Because this is a very large number (Keck has 36 segments, Hobby-Eberly Telescope has 91) we do not think it is practical to periodically install and remove these segments one at a time. As a result we have decided to handle and support the segments in groups, called clusters. We expect a standard cluster will consist of 19 hexagonal segments. Thus we will need approximately 60 clusters to make up the primary mirror. A conceptual drawing of the cluster pattern is shown in Figure 7-1. At the periphery we will use partial clusters.

A simple two-layer truss will support a cluster of 19 segments, and this truss will connect to the main part of the mirror cell at three points. The cluster truss is shown schematically in Figure 7-2. Each cluster truss will weigh roughly 745 kg and support a segment mass of 1560 kg plus segment supports. The function of the cluster is to support the segments and hold them stiffly in the correct position, and be easily installed or removed from the mirror cell below. Accuracy is important here, as inter-segment gaps are only 2 mm. The on-cluster segment positioning must be done to a modest fraction of a mm, and the cluster installation on the mirror cell must be at the same level of accuracy.

A preliminary design of the cluster truss is very stiff. It has a lowest frequency on its three support points of about 30 Hz., with displacements perpendicular to the cluster plane. The maximum gravity-driven deflections from zenith to horizon are about 0.150 mm. Details are given by Medwadowski (2001a).

Most circular
cluster layout

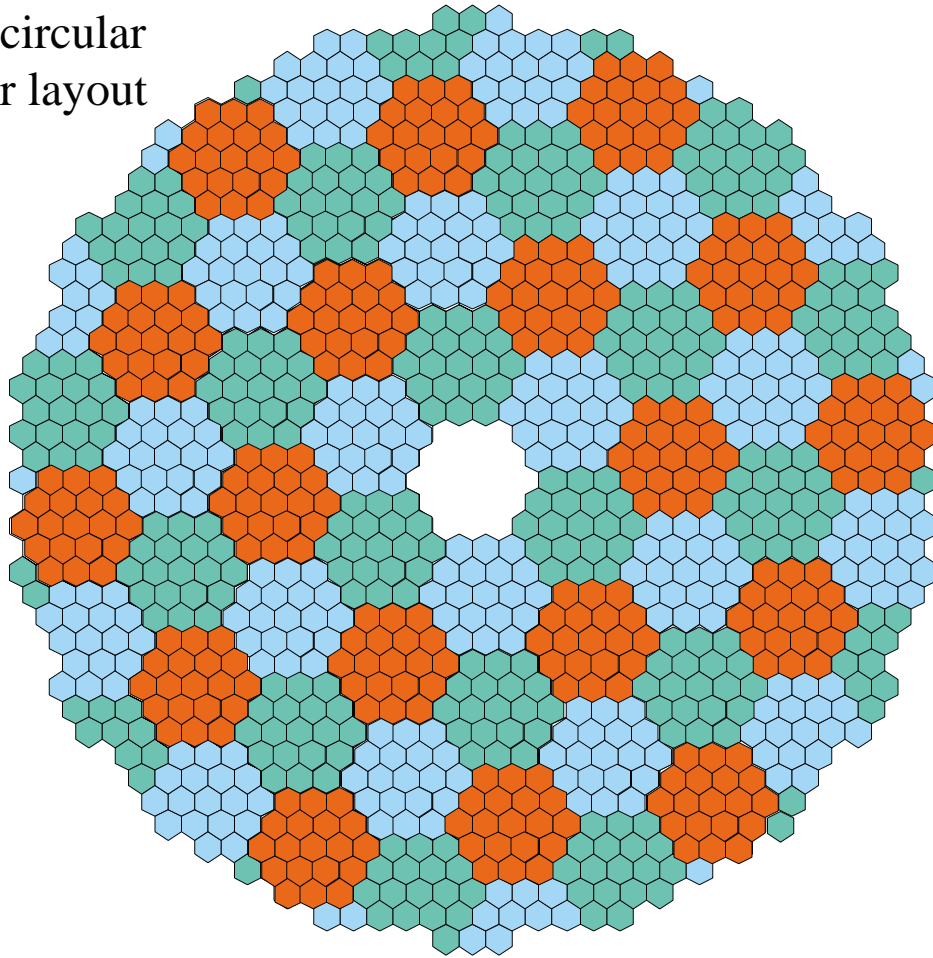


Figure 7-1. Coloring clusters in three different colors indicates the cluster pattern of the primary. Sixty clusters are used, with each cluster (typically) holding 19 segments.

At this time we have not developed the details for assembling, installing, and removing the clusters. This is an important activity for the next design phase.

7.2.3 Cell and Subcell Topology

Each segment will have a subcell with which to interface to the cluster. The subcell will hold the actuators (3/segment) and the lateral support system. The subcell will be a simple and lightweight spaceframe, similar to those used for Keck, and will weigh roughly 8 kg.

Medwadowski (2001a) has studied a subcell geometry. This loaded structure has a lowest natural frequency of 43 Hz.

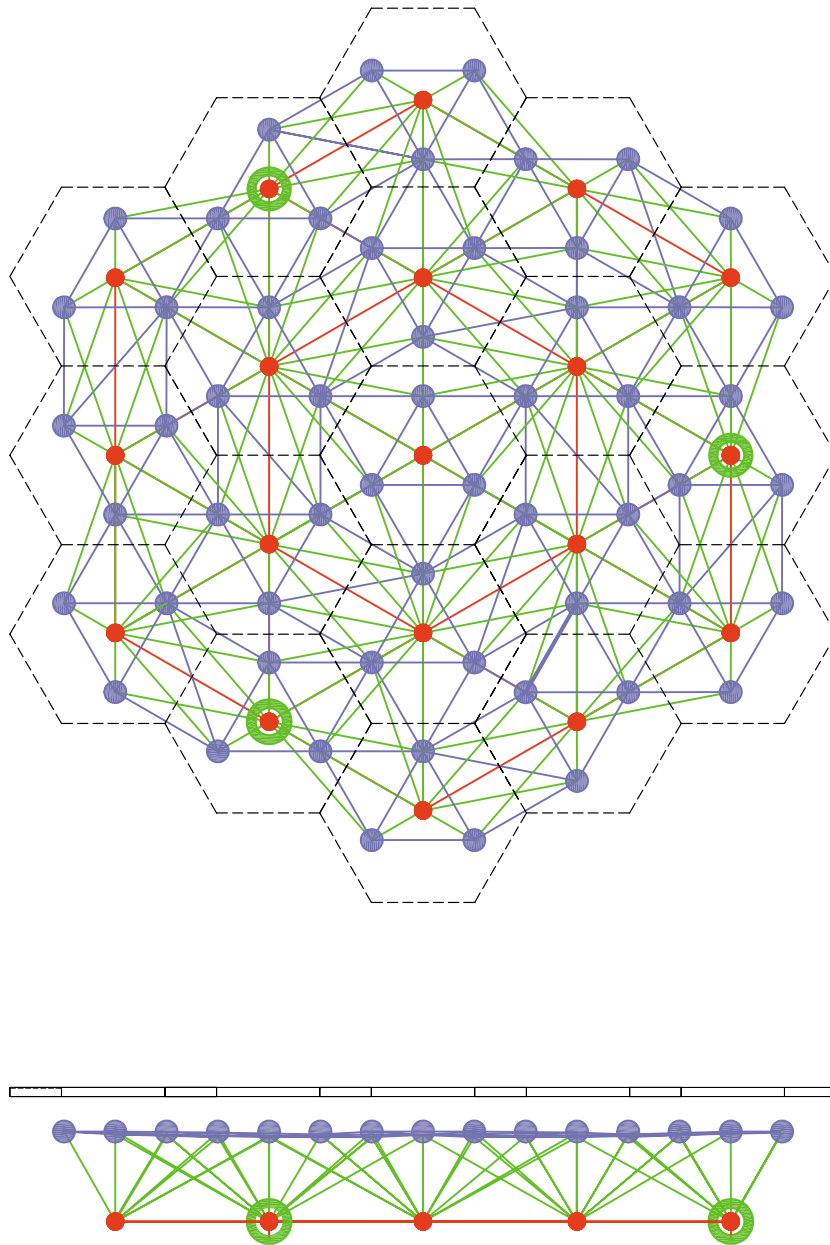


Figure 7-2. The cluster structure is shown in plan and elevation views. The blue nodes represent actuator locations in the upper layer of the truss, and blue lines interconnect them in the upper layer. Red nodes indicate the nodes of the lower layer of the structure, and red lines show the interconnection of these nodes in the lower layer. These connect all nearest neighbor nodes in this layer, although the colors of the connections are not always clear, as green diagonal members occasionally overlap them. Green lines indicate the diagonals between upper and lower layers. Three lower nodes are circles and indicate the connection to the rest of the mirror cell. The segments are indicated for scale. The segment detailed support is omitted.

7.2.4 Cell Dimensions and Performance

The design and performance of the cell and tube are described by Medwadowski (2001b, d). The cell as a whole must stiffly and accurately support the clusters at the top cell surface and must transfer the load onto elevation journals at the bottom. The elevation journals are circular arcs with centers on the elevation axis, 3.5 m in front of the vertex of the primary. A side view of the cell is shown in Figure 7-3. We can see further details of the structure with a front view of the cell, shown in Figure 7-4. The current design has two elevation journals. We have explored a system with four journals that has certain advantages, and in the next phase of work we will continue this exploration.

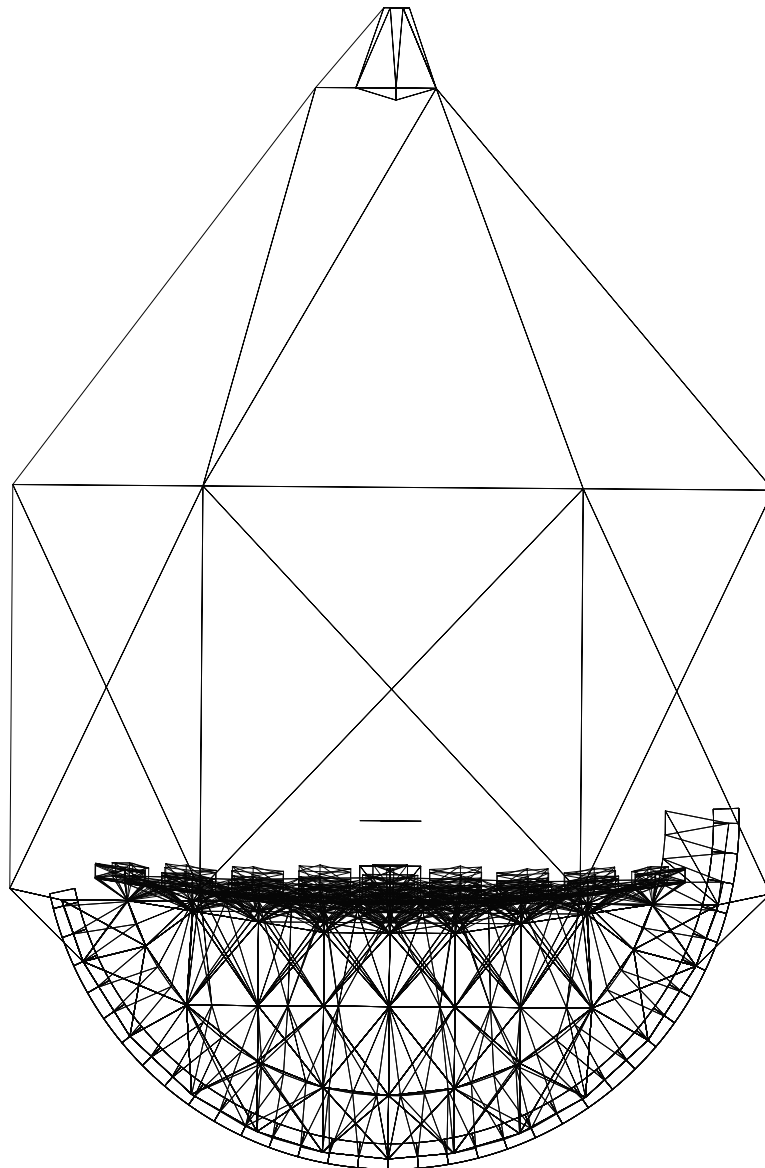


Figure 7-3. A side view of the telescope tube. The elevation journals (circular arcs) are visible, as is the mirror support cell.

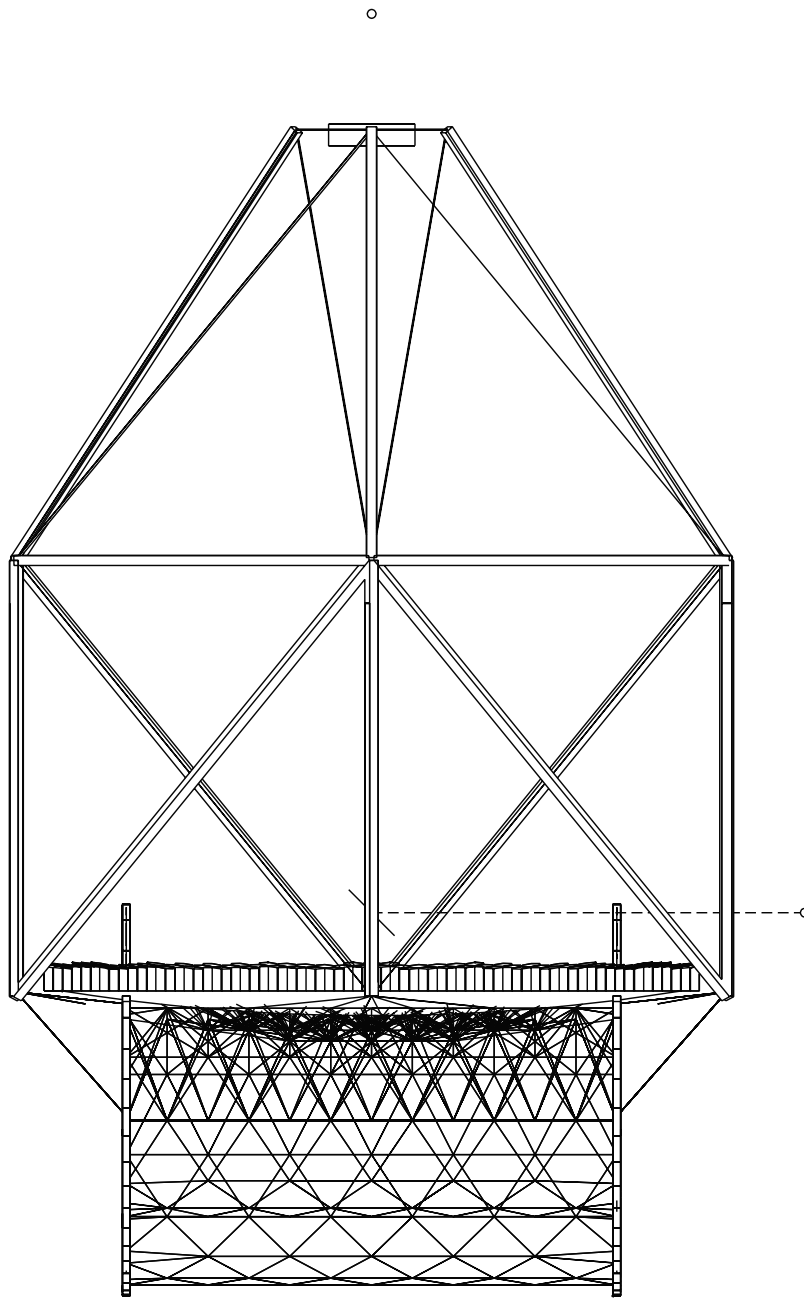


Figure 7-4. A front view of the telescope tube. This shows the mirror cell structure from another perspective.

At the top layer the scale length of the structural elements is 2.5 m (the distance between cluster attachments). As we go deeper into the cell it changes into a pattern compatible with the circular elevation journals. The characteristic structure size now becomes the size of the clusters, about 4 m, and follows a triangular structure. This can be seen in the side view of the structure shown in Figure 7-3.

The critical task of this cell is to hold the segments in the proper location against varying gravity loads. Since the subcell and cluster structure are extremely stiff, we can estimate the performance by looking at the motions of the cluster attachment points.

At the zenith, the average gravity-driven displacement along the optical axis is 2.87 mm. The peak-to-valley range about this average is 13.7 mm. This range by itself is not critical, since the optics can be aligned to the desired position for a single elevation angle. What is critical is the range of motion of each of the attachments over the elevation angle range of the telescope, since this sets the required actuator range. For Keck the corresponding motions are about 1 mm.

As the telescope moves from the zenith to 65 degrees, the primary rises towards the elevation axis by 10.7 mm. By examining deflections at several elevation angles and removing the best fitting plane at each elevation (such rigid body motions are compensated by secondary mirror motions), we can determine the maximum range of any support point. For the present design this is 2.25 mm. This sets the required range of the actuators that support the mirror segments. For Keck this is about 0.6 mm.

In-plane motions are also important. By examining the displacements of the cluster attachments at several elevation angles, we see that the average in-plane motion is largest at 65° zenith angle and is 15.2 mm in the y direction relative to the position at the zenith (z axis is optical axis, x axis is elevation axis). The peak-to-valley deviation from the mean is 3.6 mm. In the coordinate system centered on the average displaced segments, the average segment radial motion is about the same for all elevation angles and is negligible, and the standard deviation of the radial motions is also approximately independent of zenith angle and has a value of 1.0 mm. Radial motions of this size produce very small optical aberrations.

In-plane rotations of the segments about their individual centers are also optically important. For these estimates we have added the cluster rotation (as defined by its three nodes) and the rotation in the translated coordinate system (rotation relative to the center of the primary being the relevant factor). In this coordinate frame the maximum node rotation (an approximation of a segment rotation) is 2×10^{-4} radians, experienced at 65° zenith angle. By rotation we mean the angular change in direction of a line on a segment that originally passed through the center of the primary. This maximum rotation occurs for the outermost attachments.

These motions (displacements and rotations) produce image blur, a consequence of segment in-plane misalignment. The range of motions is well within the error budget for this effect developed in Chapter 11.

At this stage in the design, we are very interested in the in-plane motions, since they give an indication of the practicality of the optical configuration. With the segment misalignments found here, we can consider the possibility of different optical designs. The allowed misalignment varies as f_1^3/a^2 . Thus from the perspective of segment misalignment, we could consider segments as large as $a = 1.5$ m, or f_1 as short as 21 m.

7.2.5 Attachment to Elevation Journals

The stiffness of the elevation journals is critical to achieving adequate performance. The journal surface is attached to the rest of the mirror cell with a truss structure that follows the circular arc of the journal. It should be noted that large journal surfaces introduce structural issues that are significantly different from those of traditional telescope structures. In typical telescope elevation journals, the journal deformations are small and approximately independent of the elevation angle, since the journal is small and circular. Here the journal is only an arc of a circle, and because of its large size, it is a challenge to

make it extremely stiff. This stiffness is likely to dominate the dynamics of the telescope structure as a whole. As mentioned above, the current design has two journals, but we are also exploring designs with more journals.

The elevation journals have a radius of 17.4 m, centered on the elevation axis. They are separated from each other by 22.7 m.

7.3 Secondary Support

The challenge of supporting the secondary is to achieve maximum stiffness while minimizing the blockage of the primary. We have explored several geometrical configurations. Support structures following the design of Keck were tried, but they were massive and had large cross-sectional areas exposed to the winds near the top of the telescope. Single-layer structures were also explored, from tetrapods to pre-tensioned tripods (Medwadowski 2001b, c).

The design structure with the best overall performance is a two-layered structure. The base layer is a hexagonal cylindrical truss, outside of the optical path. The top layer consists of three compression members (square tubing, 0.46 m on a side) positioned radially over the primary, and six tension members (rectangular rod 0.038 m x 0.152 m) that connect the rim of the lower layer with three points that define the corners of the secondary mirror module. Under theoretical conditions where the mirror cell is assumed to be infinitely stiff, the upper tube structure with the secondary mirror system (assumed 10 tons) has a lowest natural frequency of almost 10 Hz. This upper tube structure is shown in side view in Figure 7-3 and 7-4. A detailed description is given by Medwadowski (2001d). Figure 7-5 shows the blockage of the primary by the upper tube.

7.4 Yoke

The yoke supports the telescope tube. The design and performance of the yoke is described by Medwadowski (2002a). The attachment between the tube and the yoke is through hydrostatic bearing pads, where the pads are part of the yoke and the journals are circular arcs forming the lower part of the mirror cell. The yoke must also rotate about a vertical axis, and four azimuth hydrostatic pads allow this motion and carry the telescope load onto the telescope pier. Another essential part of the yoke is the provision for two Nasmyth platforms to carry the scientific instruments. Each of these is a horizontal platform, approximately 15 x 32 m in size. Currently the height of the Nasmyth platform is 3.5 m below the elevation axis, the same as the primary mirror vertex. Each platform has an instrument capacity of 80 tons, and its use is described in Chapter 4. We expect multiple instruments to be located on each Nasmyth platform and each is pointed toward an articulated tertiary mirror. Thus, rotating the tertiary mirror can access multiple instruments without any motion of the scientific instruments.

In the current design there are six bearing pads supporting the tube, three under each journal. This raises an important issue that is not yet completely understood or resolved. By design the pads lie on the surface of a cylinder, centered on the elevation axis. As a rigid body, the cylinder requires six constraints to define its position, three rotations and three displacements. One rotation is the desired rotation about the elevation axis; hence the drive system provides the needed constraint. One displacement is motion along the elevation axis, which we must restrict with additional hydrostatic pads at the faces of the “cylinder.” The other four degrees of freedom are constrained by the radial bearing pads. A four-pad system (treated as points here) would properly constrain the other four degrees of freedom (two displacements and two rotations). Additional supports lead to an indeterminate support

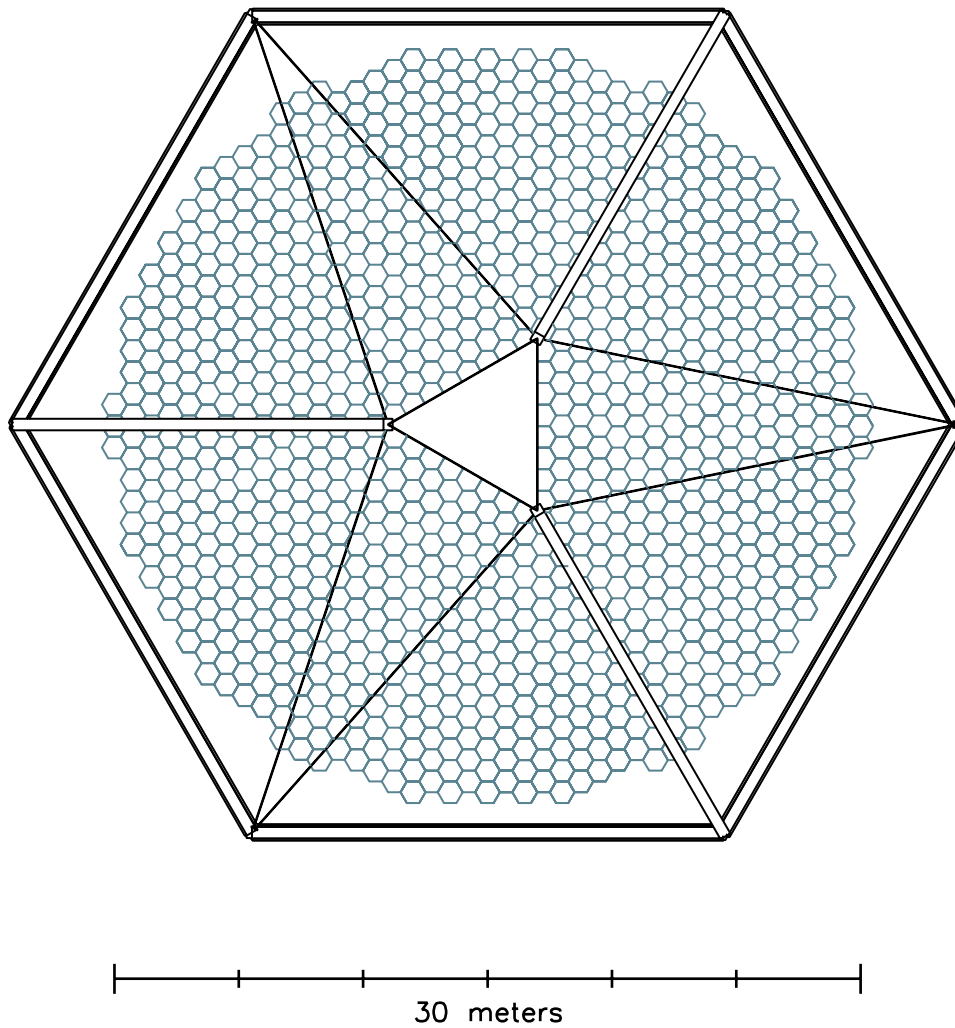


Figure 7-5. View of the primary mirror from a star, showing the blockage caused by the upper tube structure that supports the secondary mirror.

where the loads at the supports are not well defined. However, the tube structure is relatively flexible, thus for small displacement errors it will generally conform to the assumed fixed positions of the pads. Gravity loads on these six pads will be nominally constant with changing telescope zenith angle. However, journal fabrication and pad installation errors or structure temperature differences will cause these six pads to move from the desired cylindrical surface. In this case the tube structure will deform to maintain contact. The potential consequence of this is that the mirror cell will deform and additional actuator range will be needed. This is important because segment support actuators have a limited range that is difficult to increase. A four-pad system would not suffer from this concern, but a six-pad system does. This is a quantitative issue, but it may also be possible to couple two pads together so one of them can change its height as a function of pressure variations. This would restore the system to a quasi-kinematic design.

A front view of the yoke is shown in Figure 7-6. An end view of the yoke is shown in Figure 7-7. A top view of the yoke is shown in Figure 7-8. The six elevation axis bearings are indicated as small blue circles in these drawings. On each journal, two bearings are symmetrically separated by 50° while the third is placed an additional 20° along the journal. The two journals are separated by 22.7 m along the x axis.

In azimuth the four hydrostatic pads form a rectangle, 23.3m , x 22.7m. The azimuth journal surface is 25.35 m below the elevation axis. The four azimuth pads are indicated as small red circles in Figures 7-6, 7-7 and 7-8.

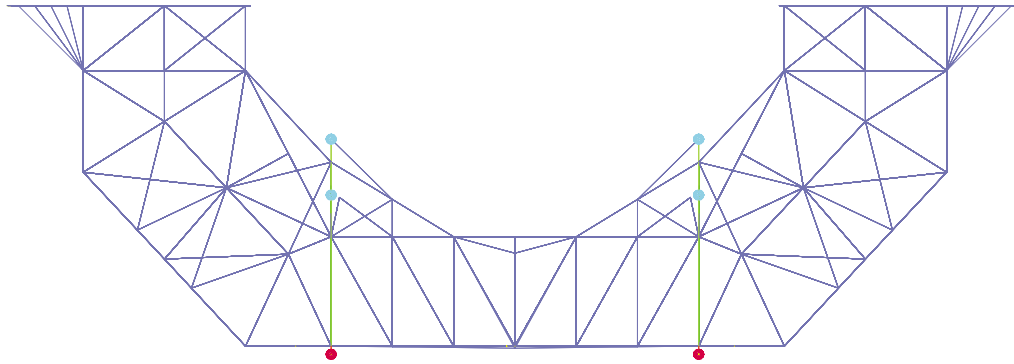


Figure 7-6. Front view of the yoke, showing the structure supporting the Nasmyth platforms and also indicating the elevation bearing pads and the azimuth bearing pads as small circles.

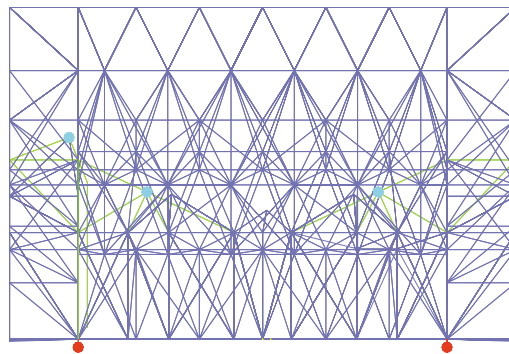


Figure 7-7. End view of the yoke, showing its structure. Again, small circles indicate the elevation and azimuth bearing pads.

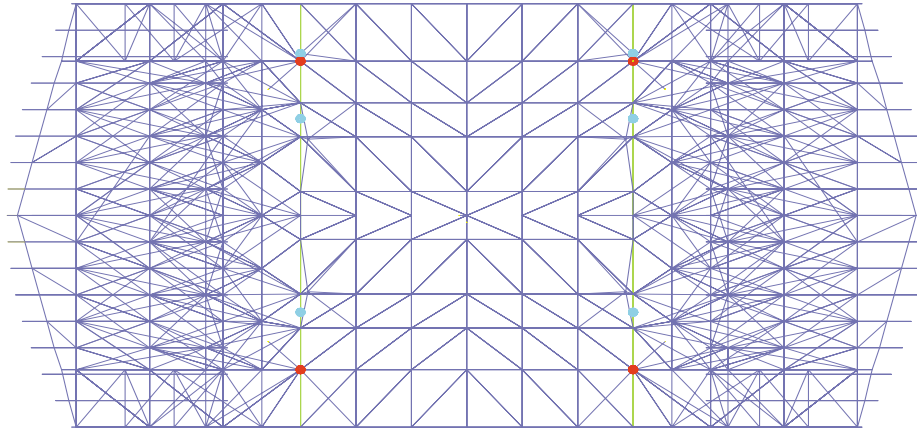


Figure 7-8. Top view of the yoke, showing its structure. Again, small circles indicate the elevation and azimuth bearing pads.

The four azimuth hydrostatic pads are designed to carry the vertical loads and will constrain three degrees of freedom of the yoke (piston, tip, tilt). Once again we are over-constrained, and will need to study the adverse consequences of azimuth journal non-flatness. The yoke will have a pintle bearing at the bottom center and this bearing will constrain the yoke against horizontal translation. This will allow rotation about a vertical axis (azimuth axis). The other side of the pintle bearing will be attached to the center of the telescope pier.

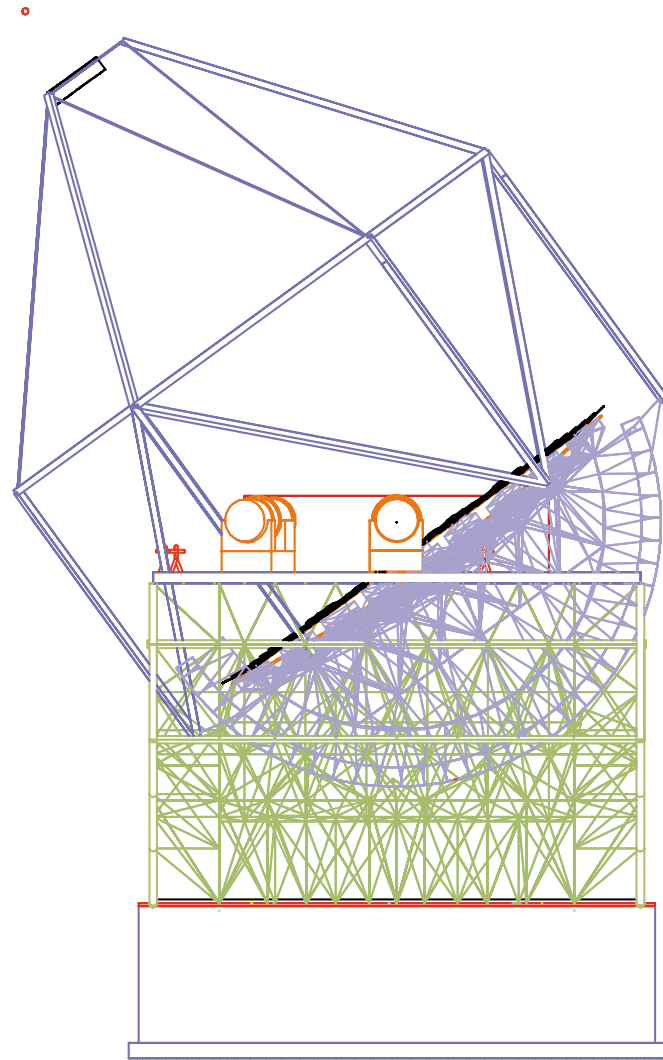
7.5 Telescope Performance

The telescope must meet a number of performance requirements: stiffness, load carrying capacity, allowed displacement tolerances, and motion control. Probably the most difficult requirements are stiffness against gravity and wind loads, and related dynamic performance. The design and performance of the integrated tube and yoke is described by Medwadowski (2002b). A side view of the telescope is given in Figure 7-9. A front view is shown in Figure 7-10, and a plan view is shown in Figure 7-11. An isometric view is shown in Figure 7-12. The masses of the telescope components are given in Table 7-1

7.5.1 Static Deflections Against Gravity

Since the telescope moves in elevation angle, the telescope must adequately hold the optics in proper alignment over the 65° range of zenith angles. It is impractical to hold the optics passively to the required tolerances. Thus, we expect that active control will be needed. The static response of the structure will dictate the range and type of active alignment control that is needed.

The first class of requirement is that the passive support of the optics should be good enough to keep the optics within the active range of adjustment. Thus the structure dictates the range of actuators that support the primary mirror segments, the actuators that control the secondary mirror position, and possibly also the system that controls the tertiary.



Observing at 54° Elevation

Figure 7-9. The telescope tube and yoke on the pier is shown from the side with the telescope at a zenith angle of 36°.

Axial displacements

As the telescope moves from zenith to 65° the primary will displace along the optical axis (z) by +10.7 mm. Analysis of the structure also shows that the secondary will displace by +15.1 mm along z in going from the zenith to 65°. Thus there is a net increase in the primary-secondary separation in going from the zenith to 65° of 4.4 mm. We expect that this correction can be done open-loop, once a lookup table of corrections has been measured. From Section 4.4.2 we see that 1 mm of axial error introduces 3.09 arcsec of defocus image blur.

In addition to axial displacements of the primary and secondary as rigid bodies, the individual segments and clusters will displace differentially. This has been analyzed in Section 7.2.4, and differential motions of segments are up to 10 mm. This can be reduced by removing the best fitting plane. The minimum actuator range for the segment actuators is set as 2.25 mm for the present design.

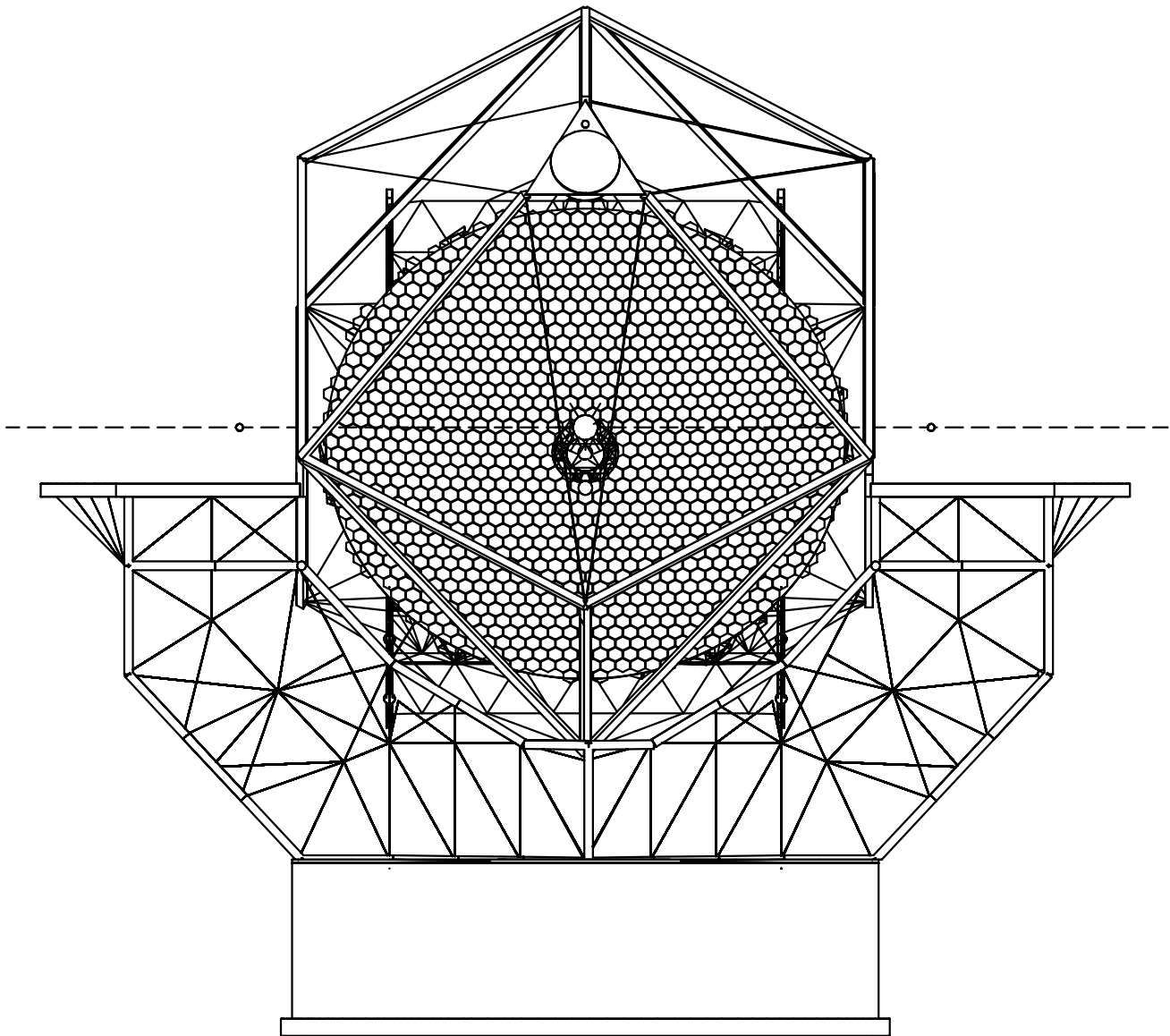


Figure 7-10. The telescope tube, yoke, and pier are shown from the front of the telescope. The telescope is at a zenith of 65° .

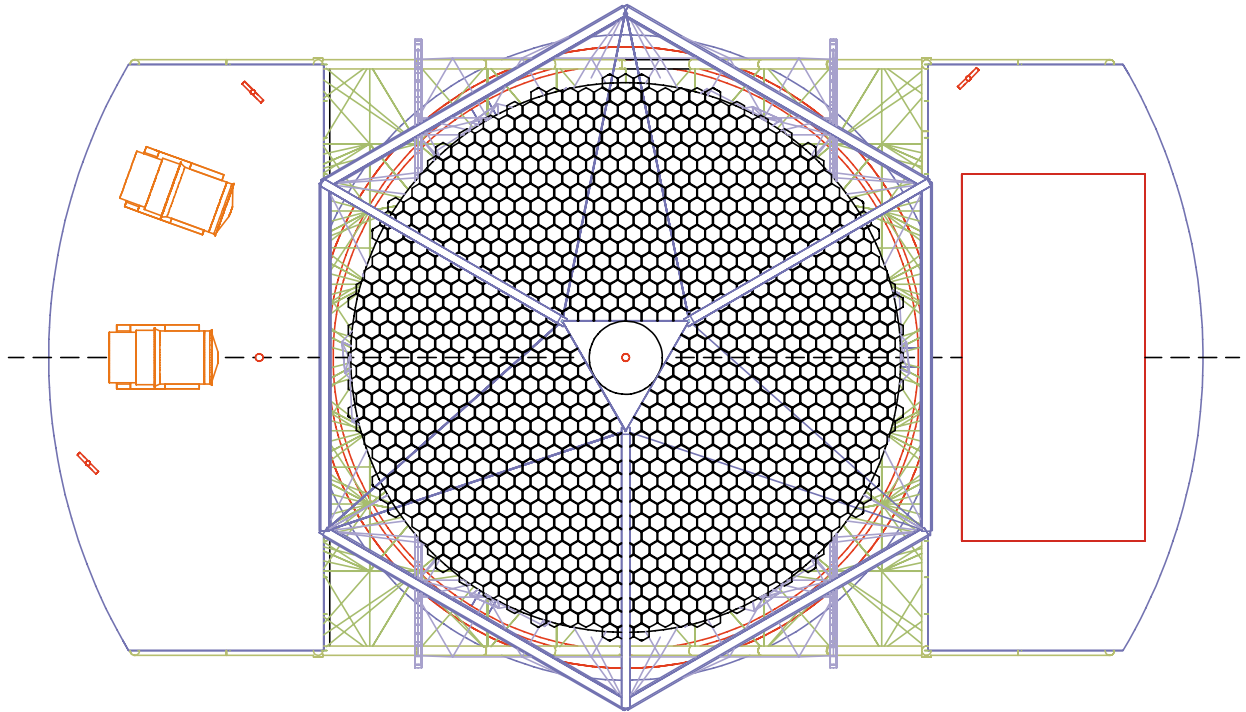


Figure 7-11. This plan view of the telescope shows the upper tube with its blockage of the primary and the Nasmyth platforms with typical instruments placed on them.

Table 7.1 Masses of key components

Component	Mass of Telescope (tons)	
Tube assembly	736	
Secondary system	10	
Secondary mirror	3.2	
Secondary support	6.8	
Upper Tube structure	152	
Tertiary mirror system	10	
Tertiary mirror	2.7	
Tertiary mirror support	7.3	
Primary Mirror system	154	
Primary Mirror	80	
Passive and active support	20	
Subcells	9	
Clusters	45	
Mirror cell and journals	410	
Yoke	440	
Nasmyth scientific instruments	160	
Hydrostatic bearings, drives	20	
Total moving mass	1356	

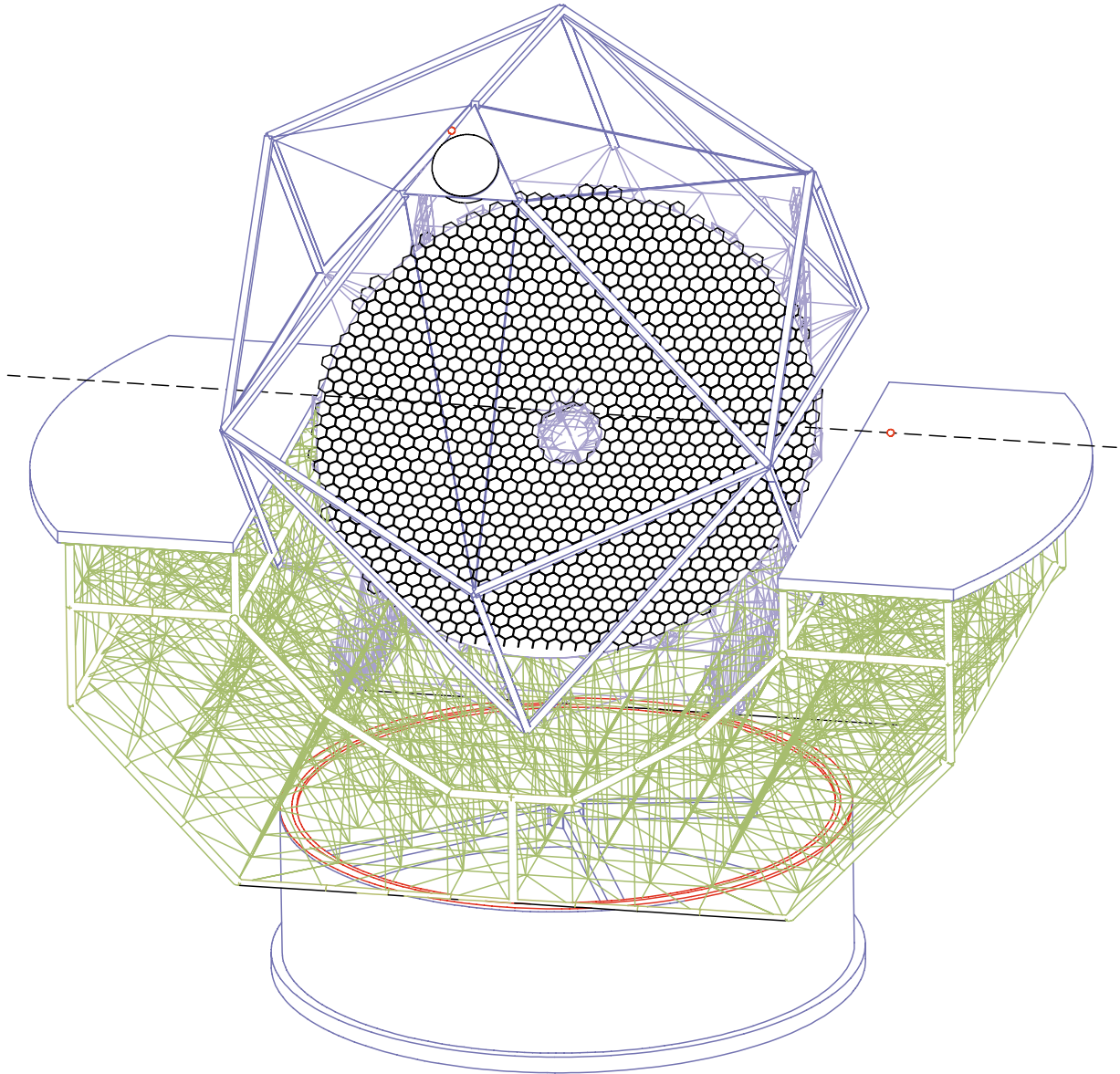


Figure 7-12. The telescope on its pier is shown, with the telescope at 30° zenith angle.

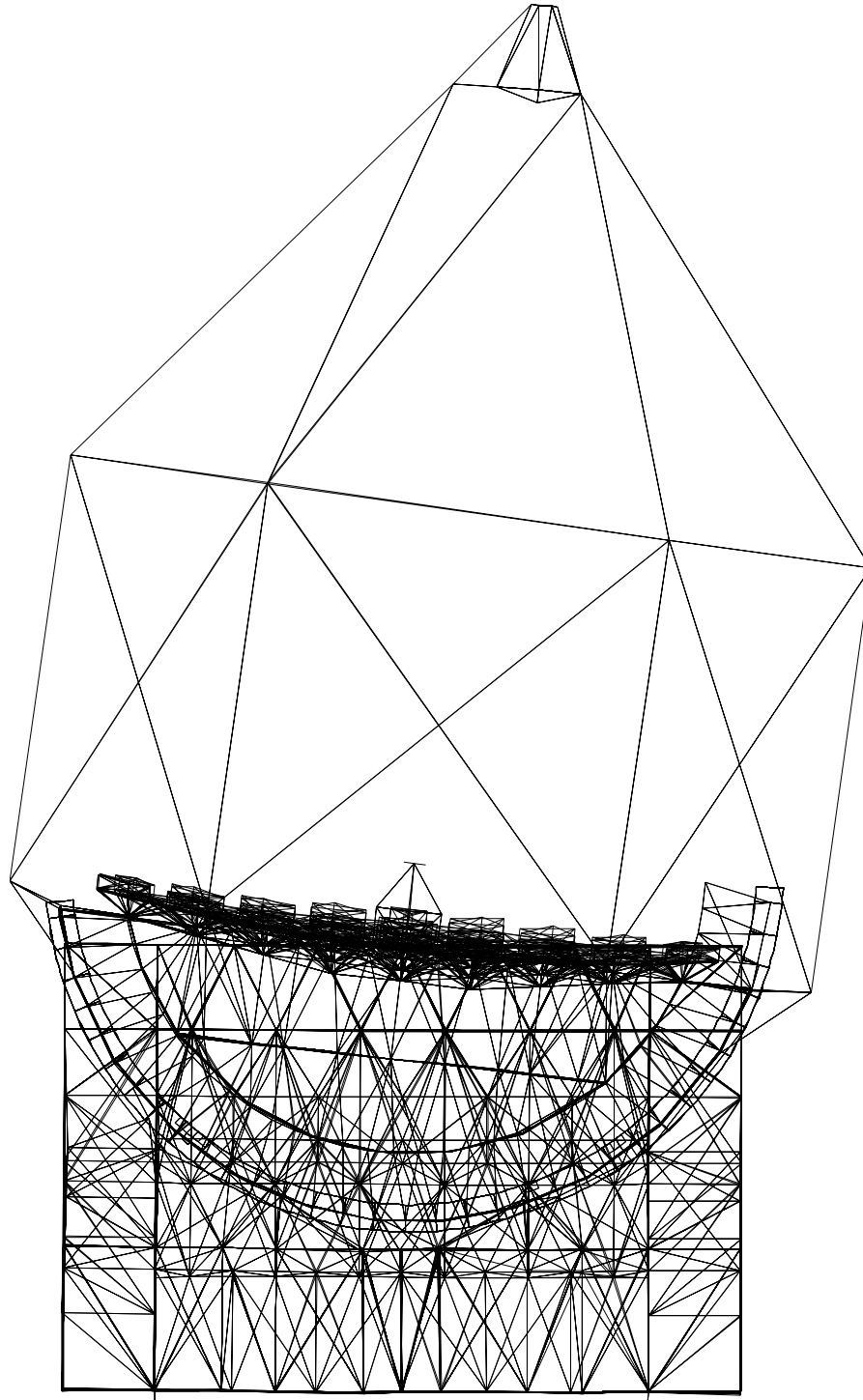


Figure 7-13. The shape of the lowest frequency mode of the telescope is shown. The natural frequency is 1.58 Hz. The amplitude is greatly enlarged to show the shape, which approximates a rotation about the elevation axis.

Lateral displacements

The decenter of the secondary relative to the primary must be controlled to a high level. As mentioned in Section 7.2.4, finite element analysis indicates that the primary mirror will laterally displace by 10.7 mm in going from the zenith to 65° zenith angle. In addition the primary will rotate by -1.09×10^{-3} radians about the x (elevation) axis in going from the zenith to 65°. This leads to a displacement of the primary optical axis at the nominal secondary position of 58.1 mm. However, the gravity driven lateral displacement of the secondary due to structural deformation is 83.1 mm, leading to a net primary-secondary decenter at 65° of 25.0 mm. We saw in Section 4.4.2 that the primary-secondary system must be in lateral alignment to about 0.1 mm. Hence the active control of the secondary position must correct the 25.0 mm to this level of accuracy. We expect that mapping out these changes and subsequently applying them open-loop (with no direct optical measurement) will be adequate, since gravity flexure is quite repeatable. At Keck gravity flexure has been measured with non-repeatability no worse than 1 part in 1000. The autoguider will also in all likelihood have wavefront sensing that can at least measure the misalignment coma and thus ensure it is cancelled closed-loop.

Relative tilts

We have indicated that the primary will rotate (tilt) by -1.09×10^{-3} radians in moving from zenith to 65°. Analysis also shows that the secondary mirror will rotate by -6.1×10^{-4} radians leading to a net secondary tilt of 4.8×10^{-4} radians. In Section 4.4.2 we saw that tilt of the secondary introduces coma at 0.010 arcsec/arcsec. Hence this rotation will introduce 1.02 arcsec of coma. We expect that we will actively correct all secondary position and angle errors.

These rigid body motions will be included in the telescope pointing system, and also in the primary-secondary alignment system.

The relatively large static deflections of the properly aligned primary-secondary system will cause the images to move in the focal plane, but these will automatically be removed by the guiding system. In addition, translations of the primary-secondary optical system relative to the elevation axis can cause a tilt of the focal plane. Assuming a displacement of 20 mm, and assuming the tertiary is tilted to stabilize the image at the instrument, we will tilt the focal plane by the ratio of the displacement divided by the distance to the tertiary, or $0.020/20 = 0.001$. At the edge of the 20-arcmin field of view, this will cause a defocus of 0.04 arcsec, an acceptably small value.

A second class of static misalignments is connected to the in-plane segment misalignments. As mentioned in Section 7.2.4, gravity will cause the segments to both translate and rotate in the coordinate system of the primary mirror. The gravity displacements must not exceed the error budget given in Chapter 11. If these exceed the requirements we have several options. We must either introduce active control to these motions: modify the structural design to reduce them, modify the optical design (smaller segments, longer primary focal length) to relax the tolerances, or use warping harnesses to actively change the shape of the segments as a function of elevation angle. As stated in Section 7.2.4, the present design is adequate in this regard.

7.5.2 Static Deflections Against Wind

Wind loads on the enclosure and telescope are a potential problem on windy nights. The details of these wind loads will be site dependent and enclosure design dependent, so quantitative results are not available at this time. Further, the wind loads will have a significant dynamic component; hence static

estimates of the effect of wind loads do not adequately define the problem. Nonetheless, static estimates give one a useful basis for understanding the magnitude of the problem.

The shielding value of the enclosure is extremely important. For Keck Observatory, wind tunnel tests were made of the dome and shutter. The wind speed reduction was measured at a variety of locations within the interior of the dome for a variety of dome elevation and azimuth values. Kiceniuk and Potter (1986) give the detailed reports of this study. The Keck dome geometry is very close to that of the CELT enclosure design (see Chapter 12); the Reynolds numbers are very high in the wind tunnel test ($Re > 10^6$) so the measurements should be applicable to CELT.

The measurements are made at a range of distances from the dome center. For CELT the secondary mirror is located at a distance of 35.9 m from the dome center, or 0.798 of the dome outside radius of 45 m. Kiceniuk and Potter made many measurements at a radius of 0.815 of the dome outside radius, so we will use these results herein. They find that at this radius the interior air circulates in a rotational sense, i.e., the air motion is tangential to the dome surface. Further, the absolute worst case they found among all telescope orientations was that the inside air speed was reduced to 30% of the outside free air speed. In all downwind directions, the highest wind speed was 11% of the free air speed. Other measurements were made at a variety of radii. It was found that the residual interior velocity is a rapid function of how deep in the dome one makes the measurement. At the equivalent CELT radius of 40.0 m they find the dome shielding is less effective, with a worst case wind reduction to about 0.46 of the outside free air speed.

There is anecdotal experience at Keck Observatory that is consistent with these wind tunnel results. Observers have complained about telescope shake on very windy nights when pointing upstream into the wind. However, the normal Keck shutter configuration has the shutters fully open. When the shutters were closed to the minimum opening, indications of telescope shake from wind disappeared. From this we can conclude that setting the shutter to its minimum opening (the configuration of the wind tunnel tests) has a significant shielding effect from the wind. More recent tests of the effects of wind have been undertaken for the Gemini enclosure in Chile (Gemini 2000). Similar attenuation factors were found.

Given this data, we can make some rough estimates of wind loads on CELT. We make a very conservative assumption that the wind reduction at the top end of CELT will be 0.40. In reality, observers typically work at orientations that are random with respect to the wind direction; thus one might average the wind reduction factors instead of picking the worst case. We have chosen an attenuation value between the above stated 0.30 and 0.46 to account for the fact that the secondary structure will have a range between 35.9m and 37.9m.

We select the wind statistics of Mauna Kea to work out an example. At Mauna Kea the wind is in excess of 12m/s 10% of the time (Nelson, et al., 1985). Thus we will assume that in these wind conditions the wind speed at the top end of the telescope is 5m/s. Further, we assume that the wind speed drops linearly to zero at the center of the dome. The wind tunnel data indicate that the wind speed drops more rapidly than linear as one goes inwards from the dome edge, hence this is also a conservative assumption.

The static force on the telescope is given by

$$F = \rho v^2 C_D A / 2 \quad (7-4)$$

where $\rho = 0.764 \text{ kg/m}^3$ the density of air at the site (assumed Mauna Kea)

$v = 5\text{m/s}$ the wind at the top of the telescope

$C_D = 1$ the drag coefficient of the wind on the structural element (typical)

A = cross section of the element.

The drag coefficient is a function of the shape of the element and the Reynolds number (Re) of the airflow past the element. For flat plates $C_D = 2$ is reasonable, but for cylinders it is roughly 1 for $\text{Re} < 250000$ and 0.5 for $\text{Re} > 250000$. Thus the shape of the elements can have a significant impact on the net wind force.

For our example, the telescope at the top end will experience static wind pressures of 9.5 N/m^2 (assuming $C_D = 1$).

To estimate the impact on the telescope, it is more relevant to calculate the net torque on the telescope, given the variable wind speed as a function of height along the telescope. We can then calculate the force at the top end that provides this torque, and the secondary mirror motion, and the resulting image motion. This takes advantage of the numerical results of the deflections of our telescope model given a point load at the secondary.

Using the upper tube model described by Medwadowski (2001b), we calculate the effective cross sectional area (weighted by the wind speed squared and the moment arm) to be 21.7m^2 . The Medwadowski telescope model (2002b) produces an effective spring constant for lateral displacements at the secondary of $1.04 \times 10^7 \text{ N/m}$. Combining the pressure, the effective area and the spring constant yields a static wind deflection at the secondary of $1.99 \times 10^{-5} \text{ m}$. Using the decenter-generated image motion arrived at in Chapter 4 ($4.13\text{e} \times 10^3 \text{ arcsec/m}$), we get the final estimated image motion from a static wind of 0.082 arcsec .

This image motion is a rough estimate of what might happen for the 10% external wind, not the average image motion due to wind. Thus, unless dynamics grossly alter this result, we believe this static stiffness will be acceptable. We also believe that with additional design effort the structure can become both stiffer and have a higher natural frequency. Padin and MacMartin (2001) have carried out an independent wind assessment that is consistent with the above discussion.

7.5.3 Dynamics

The dynamic response of the telescope structure is important for several reasons. First, it is a convenient metric for the stiffness of the telescope against various loads, from wind to earthquakes. Second, the lowest natural frequencies will dictate how rapidly the telescope can be moved and controlled. Third, the lowest natural frequencies will dictate how quickly we can move the secondary mirror to remove unwanted image motion. Finally, the dynamic coupling of the wind or other seismic disturbances (vibration) to the telescope depends critically on the natural frequencies, and if sufficiently excited, telescope vibrations will be detrimental to image quality. In all respects, we want a telescope with the highest practical natural frequencies.

The present design of the telescope structure has dynamics that depend sensitively on the elevation angle of the telescope. For a wide range of elevation angles ($\text{el} > 40^\circ$) from the zenith, the behavior is essentially the same as at the zenith. For this range, the lowest natural frequency is about 1.6 Hz. As the zenith angle nears the 65° limit, the performance degrades significantly; and the lowest natural frequency drops to about 1.2 Hz. The lowest modes appear to involve the elevation journals in a significant way, approximating a rocking motion in the y-z plane. The x axis is along the elevation axis. Figure 7-13 shows the distortion in the lowest mode at the zenith.

The lowest mode at the zenith has a natural frequency of 1.58 Hz, and the shape corresponds approximately to rotation about the x axis, with the deformations largely those of the elevation journals. The second mode occurs at 1.85 Hz and appears largely as rotation about the y axis (rocking motion in the x-z plane), with shearing of the journal-mirror support structure. At 65° the mode shapes are similar to the zenith, but the frequencies are 1.16 Hz and 1.59 Hz.

In the next phase of work we will study more carefully the reasons for these low natural frequencies with the hope of improving them. They may be a fundamental consequence of the large elevation journals.

7.6 Pier

The yoke is supported on hydrostatic bearings that move on an azimuth journal. This journal radius is 16.26 m. Because of the large size of the telescope, we see little benefit in elevating the telescope. As a result the azimuth journal will be about 1 m above the ground, a height convenient for maintenance. The total mass of the tube, the yoke, and the scientific instruments will be 1356 tons, and is carried by four azimuth pads to the journal at the top surface of the pier. The pier will be rigidly connected to the earth, relying largely on the mass of the pier. We expect that the pier mass will be about 10 times the mass of the telescope, or 10^4 tons.

The pier shape is shown in Figure 7-10. It is roughly an inverted mushroom with a stiff base disk and a cylinder attached to it. The cylinder depth will be set by the soil conditions, assumed here to be 10 m. A wall thickness of 0.7 m should be adequate. The interior of the pier will be filled with sand or some other dissipative material. The concrete mass will be approximately 3715 tons, and the interior fill will have a mass of roughly 15000 tons.

In Section 7.5.2 we saw that wind loads on the top end of the telescope could be an important issue. In addition to deforming the telescope structure, wind loads will exert a torque on the pier and in turn on the soil under the pier. To estimate the magnitude of this effect we assume we can treat this situation as a disk on a semi-infinite elastic foundation (Richart, et al., 1970).

If the telescope were pointing to the horizon, there will be a rotation about a vertical axis that is given by

$$\theta_s = 3 \tau_\theta / (16Gr_0^3) \quad (7-5)$$

where τ_θ = torque about vertical axis = 7380 Nm

G = soil shear modulus = 4.82×10^7 N/m² (for Mauna Kea, Harding-Lawson, 1986)

r_0 = radius of pier = 17 m

yielding $\theta_s = 0.0012$ arcsec

The other extreme is when the telescope is pointing to the zenith and the foundation rotates about a horizontal axis. In this case

$$\theta_s = 3(1 - \nu) \tau_\theta / (8Gr_0^3) \quad (7-6)$$

where ν = Poisson ratio of soil = 0.3

$$\tau_\theta = 12510 \text{ Nm}$$

yielding $\theta_s = 0.0029$ arcsec

We conclude that the additional influence of the wind on the telescope rocking the telescope pier is small. Nelson (1983a) and Medwadowski (1984) describe different analytical approaches to this issue.

7.7 Bearings

The telescope motion is most efficiently handled using hydrostatic bearings for both axes. Hydrostatic bearings support very large loads, have extremely small drag and stiction, and are extremely stiff. Their major concerns are the necessity of handling liquid oil and avoiding consequent vibrations introduced by the oil pumps. A conceptual study of CELT bearing options and the characteristics of a hydrostatic system in particular was carried out by Vertex RSI (2001).

The vertical load on the elevation bearings is 736 tons, and with an opening angle of 50° , each of four bearing pads must carry a load of 1.99×10^6 N. With six elevation bearings the load distribution will be different, but we will not explore the details here. Assuming that the hydrostatic bearing oil is supplied at a pressure of 1.0×10^7 N/m² (1450 psi) each of the elevation pads needs an effective area of 0.20 m². The four azimuth pads carry a total load of 1356 tons, thus each pad must carry a load of 3.33×10^6 N. Assuming the same oil pressure as the elevation pads, each azimuth pad needs an effective area of 0.33 m².

As the telescope moves, oil must be supplied at a sufficient rate that the pads do not overrun the oil during slewing. To meet our slew requirements ($>1.2^\circ/s$ az, $0.22^\circ/s$ el), the pads must move relative to the journal at up to 0.36 m/s (0.064 m/s el). This implies the flow rate to the set of pads (assuming an oil thickness of 50 μm) must be at least 1.42×10^{-4} m³/s (2.14×10^{-5} m³/s el). The total oil flow is thus 1.63×10^{-4} m³/s (9.8L/minute).

The hydrostatic oil heats up as it exits the pad ($\Delta T = p/c\rho$). To avoid adding heat to the dome volume, the oil should be precooled by about 7.0°C . This will allow the oil to exit at the ambient temperature. The thermal power is about 1.6 kW.

One of the virtues of hydrostatic bearings is their extreme stiffness. With a film thickness of 50 μm , the stiffness is 6×10^{10} N/m, orders of magnitude stiffer than the telescope structure. Pumps and cooling systems with these capacities are routinely available, so we foresee no unusual problems with the use of hydrostatic bearings on CELT.

As mentioned earlier, the lateral restraint of the yoke will be a pintle bearing at the center of the yoke. This bearing will be a rolling element bearing and by design will only carry horizontal loads. In elevation, motion along the elevation axis will be constrained by additional hydrostatic bearings, a technique used successfully on Keck.

7.8 Drives and Encoders

The drive system for the telescope must meet the slew requirements and also move the telescope smoothly enough for scientific observations. Vertex RSI (2001) studied several drive systems including wheel and track, direct drive (used on the VLT), and gear driven drives. They recommend that a gear driven system can economically meet our requirements. To meet our slewing requirements (acceleration requirements) they recommend 4 x 37 hp motors in azimuth, and 4 x 8 hp motors in elevation.

Geared systems may introduce ripple into the response, which is undesirable. However, with pairs of motors opposing each other, hysteresis and backlash can be prevented, and with modern controls and suitable encoding, smooth performance can be achieved. Helical gears are suggested as excellent candidate gear systems because of their relatively uniform contact area. Helical gears are being used on Southern Astrophysical Research Telescope (SOAR, 2001), with excellent results.

In azimuth the gear is likely to be part of the pier/journal system while two pairs of opposed motors will be attached to the yoke. In elevation the gears will be attached to the two journals, and the two pairs of motors will be attached to the yoke. Dynamic analysis by Vertex RSI indicates that all the dynamic motion requirements can be met with such a system.

Various encoder systems can be envisioned. Again, Vertex RSI explored several encoder options, and there were several possible solutions including Heidenhain tapes, Farrand-Inducosyn, and BEI absolute encoders. Different systems have different strengths and weaknesses, but adequate encoders do exist for CELT. Other less conventional systems such as inertial reference units may also have a useful role in CELT. In azimuth there is a complete circle and also a pintle bearing, so the encoding issues are straightforward. In elevation there is only an arc of a circle; hence the encoding is potentially more difficult. Vertex RSI has suggested that the use of Heidenhain tapes (common on other telescopes) would be sufficient for our needs. These tapes give ample resolution, providing up to 0.0004 arcsec resolution (but deformations of the journals might limit their accuracy).

7.9 Thermal Responses

The telescope system must work successfully in varying thermal environments. Such variations include a wide range of static temperatures, diurnal variations, and local temperature variations across the structure. Variations in the average temperature from -2°C to $+6^{\circ}\text{C}$ (for Mauna Kea, this covers 90% of the time) should not cause any difficulties.

As mentioned at the beginning of this chapter, temperature change, temperature gradients, and more complex temperature variations will cause deformation of the structure and motions of the supported optics. These are critical issues to be explored more fully in the next stage of design. The rough estimates made currently suggest that with the planned active control of the optics, these effects will not be a problem.

The telescope structure also has significant heat capacity; hence its temperature will not perfectly follow the ambient air temperature inside the dome. These temperature differences will produce some temperature variations in the surrounding air, and thus degrade the seeing. At 1.5×10^6 kg, the telescope structure has a heat capacity of 7.05×10^8 J/ $^{\circ}\text{C}$ and must dissipate 195 kW to cool by 1°C in one hour. The entire dome air mass is only $\sim 3 \times 10^5$ kg with a heat capacity of 3×10^8 J/ $^{\circ}\text{C}$. This indicates a central issue to be addressed in the next design stage: how one causes the telescope structure to follow

the changing ambient air temperature or isolate the thermal mass of the structure, so that its skin temperature stays within about 0.5°C of the ambient air temperature.

7.10 Instrument Changing System

We plan to locate all scientific instruments on the Nasmyth platforms. With an articulated tertiary, the science light will be directed to the chosen instrument by moving the tertiary. Thus, there will be no need to routinely transport the instruments. We expect that the instruments will be mounted/assembled on the Nasmyth platforms and will be permanently stationed there. Servicing will be done in place, or key components will be removed and transported to laboratory space in the support building.

An elevator will be available to transport moderate-sized objects in support of instruments. The location of the elevator will be determined in the next phase of design. It may be stationary, as at Keck, and the telescope must be positioned suitably to allow transfer, or it might be a part of the telescope itself.

More serious instrument installation and handling will be by cranes. We expect that the dome will have a 5-ton crane, and expect that a mobile crane with over 20-ton lift will also be available at the observatory. This should be sufficient for instrument assembly and major servicing.

7.11 Segment Handling

A critical part of CELT is its 1080-segment primary mirror. We will need to install and align these segments, regularly clean them in place, and periodically remove them to be re-coated. With this many segments these processes must be carefully understood and optimized to avoid excessive effort, loss of night time, or the introduction of any significant risks to the segments themselves.

As mentioned earlier, we plan to place segments in clusters of 19, and the segment relative alignment will be set within the cluster. Thus a facility in the support building will be needed to assemble, align, and disassemble individual clusters.

Segment cleaning in place will likely be done with CO₂, which has worked well at Keck. At Keck this is done manually from a crane. At CELT, a more automated system is desired and will be developed in the next phase of work.

Cluster installation and removal is still a major issue. At Keck, segments are handled individually with a custom crane, but it has proven to be time consuming and also causes the loss of some night time. For CELT we need to develop a more convenient system, and this will be a major task in the next design phase. We expect that the wavefront sensing system for CELT will provide rapid realignment of segments by making more measurements in parallel, so that nighttime losses will be minimal.

7.12 IR Design Considerations

In the thermal IR wavelength region ($> 2 \mu\text{m}$), the emission of the telescope itself can be a significant source of background light to the scientific instruments. Proper baffling of the instrument will greatly reduce this, and only the upper tube structure is likely to be of key importance, since parts of it are directly in the optical path. When appropriate for the instrument, these parts can be blocked by a cold pupil stop in the instrument. By keeping the blockage to a minimum, we expect the structure will not be a major background source in the IR. It appears that the segment gaps and edges are likely to be a

difficult-to-remove source of background, a phenomenon fundamental to segmented mirror telescopes. As mentioned in Chapter 4, the segment gaps and edges constitute about 0.9% of the primary mirror area.

7.13 Control of Secondary and Tertiary

In Chapter 6 we discussed the secondary and tertiary controls. We plan to actively control the rigid body motion of the secondary. In addition, the secondary will have an active support system that can change the secondary shape. We expect this will be used to set and stabilize the secondary surface shape. The tertiary will have active control over two rigid body motions, rotations about the z axis, and rotation about the local y axis. None of these controlled motions are expected to have significant dynamic impact on the telescope structure, and although the attachments have not been worked out, we expect this will be a straightforward interface.

We want to actively control the secondary mirror to reduce undesired image motion (windshake) and to chop the secondary to improve IR performance. These will be engineering challenges: rapidly and accurately tilting a 10-ton object, and minimizing the dynamic interactions with the rest of the telescope. In the next phase of work we will address these challenges. Engineers responsible for large chopping secondary mirrors on Keck and Gemini have expressed optimism that this is practical at the 1 Hz level (Lorell 2001).

7.14 Field Rotation and Other Effects of Alt-Az Mount

An altitude-azimuth telescope has structural advantages, but it adds an astronomical complication. The scientific field of view rotates relative to the telescope as the telescope motion removes the star motion caused by the earth rotation. This field rotation is generally harmless when a single star is being studied, but when an extended object or region is being studied, this rotation must be removed. In addition, the telescope motions in azimuth become infinitely rapid as the observing region approaches the zenith. Thus there is an effective blind spot near the zenith. More generally, the motions of the telescope about the elevation and azimuth axes are variable, even though the Earth's rotation rate is constant.

Nelson (1981) describes the quantitative aspects of telescope and field rotation. The additional motion of the tertiary needed to keep a star image on a given instrument at any location on the Nasmyth platform is described by Kuhlen (2001). There are no singularities or other unusual motion requirements of the tertiary.

REFERENCES

Gemini South 8-m Optical Telescope, Final Report. Modal Analysis and Controls Laboratory Report No. -05-08570-001. CD-ROM produced by David R. Smith: "Wind Tests Data from Gemini South." May 13-14, 2000. Mechanical Engineering Department, University of Massachusetts: Lowell, Massachusetts.

Harding Lawson Associates. 1986. "Soil Investigation Keck Observatory 10-m Telescope, Mauna Kea, Hawaii." Keck Observatory Report No. 152.

Kiceniuk, Taras and Kent Potter. 1986. "Internal Air Flow Patterns for the Keck 10 Meter Telescope Observatory Dome." Keck Observatory Report No. 166.

Kuhlen, Michael. 2001. "The Tertiary Mirror Equations of Motion of an "off-altitude axis" Nasmyth Focus." CELT Report No. 22.

Lorell, Ken, 2001, private communication.

Medwadowski, Stefan J. 1984. "UC telescope pier rotations due to wind action on the observatory dome." Keck Observatory Report No. 53.

Medwadowski, Stefan J. 2001a. "The structure supporting a cluster of segments of the primary mirror of CELT." CELT Report No. 25.

Medwadowski, Stefan J. 2001b. "The structure of the tube of the CELT telescope." CELT Report No. 26.

Medwadowski, Stefan J. 2001c. "CELT tube structure with upper tube in the form of a tripod-on-hexagon." CELT Report No. 27.

Medwadowski, Stefan J. 2001d. "CELT Tube Structure, Final Conceptual Design." CELT Report No. 28.

Medwadowski, Stefan J. 2002a. "CELT Yoke Structure, Final Conceptual Design." CELT Report No. 29.

Medwadowski, Stefan J. 2002b. "CELT Structure (Tube on Yoke), Final Conceptual Design." CELT Report No. 30.

Meinel, Aden and Marjorie Meinel. 2000. "Configuration Options CELT." CELT Report No. 31.

Nelson, Jerry. 1981. "Geometrical Relations for an Altitude Azimuth Telescope." Keck Report No. 49.

Nelson, Jerry. 1983a. "Telescope pier rotation from wind loads on building and dome." Keck Technical Note No. 58.

Nelson, Jerry. 1983b. "The effects of wind loads on the ten meter telescope." Keck Report No. 47.

Nelson, Mast, and Faber. 1985. "The Design of the Keck Observatory and Telescope." Keck Observatory Report No. 90.

Padin, Steve and Doug MacMartin. 2001. "Aberrations due to wind-induced secondary decenter in CELT." CELT Technical Note No. 24

Richart, F. E., J.R. Hall, Jr., R. D.Woods. 1970. *Vibrations of Soils and Foundations*, Prentice-Hall.

SOAR, <http://www.soartelescope.org/>, 2001.

Vertex RSI. October 2001. "30-m CELT Telescope Drives, Bearings and Encoder Study." CELT Report 21.

von Hoerner, Sebastian. 1967. *Astronomical Journal* **72**, 35.

